Nigmatullin, R., Gabrielli, V., Muñoz-García, J. C., Lewandowska, A. E., Harniman, R., Khimyak, Y. Z., Angulo, J., & Eichhorn, S. J. (2019). Thermosensitive supramolecular and colloidal hydrogels via self-assembly modulated by hydrophobized cellulose nanocrystals. *Cellulose*, *26*(1), 529-542. https://doi.org/10.1007/s10570-018-02225-8

Thermosensitive supramolecular and colloidal hydrogels via self-assembly modulated by hydrophobized cellulose nanocrystals

Rinat Nigmatullin[1], Valeria Gabrielli[2], Juan C. Muñoz-García[2], Yaroslav Z. Khimyak[2], Jesús Angulo[2], Stephen J. Eichhorn[1,*]

1. *Bristol Composites Institute (ACCIS), University of Bristol, Bristol, BS8 1TR, UK*
2. *School of Pharmacy, University of East Anglia, Norwich Research Park, Norwich, NR4 7TJ, UK*

Abstract

Utilization of reversible non-covalent interactions is a versatile design strategy for the development of stimuli responsive soft materials. In this study, hydrophobic interactions were harnessed to assembly water-soluble macromolecules and nanoparticles into a transient hybrid network forming thermosensitive hydrogels with tunable rheological properties. Hybrid hydrogels were built of biopolymer derived components: cellulose nanocrystals (CNCs), nanoparticles of high aspect ratio, and hydroxypropyl methylcellulose (HPMC). To enable polymer/CNC assembly *via* hydrophobic interactions, the surface of highly hydrophilic CNCs was modified by binding octyl moieties (octyl-CNCs). The amphiphilicity of octyl-CNCs was confirmed by surface tension measurements. The molecular and particulate amphiphiles assemble into hybrid networks, which result in stiffer and stronger hydrogels compared to HPMC hydrogels and hydrogels reinforced with hydrophilic CNCs. Hybrid hydrogels retain the ability of HPMC hydrogels to flow under applied shear stress. However, significantly higher viscosity was achieved for HPMC/octyl-CNC compared with HPMC/CNCs hydrogels. The inherent thermal response of rheological properties of HPMC hydrogels was further amplified in combination with octyl-CNCs due to temperature-induced polymer/nanoparticle association *via* hydrophobic interactions. Saturation transfer difference (STD) NMR spectroscopy demonstrated the growth of network-bound water with an increase in temperature, which correlates with the increase of stiffness and viscosity of hydrogels upon heating. Rheological properties of these hybrid hydrogels are defined by the content of the soluble polymer and the CNCs, and it is shown that they can be finely adjusted for a required application.

* Corresponding Author: (S.J. Eichhorn) s.j.eichhorn@bristol.ac.uk; Ph: +44 (0) 117 33 15650.

Keywords *Cellulose nanocrystals, Hydroxypropyl methylcellulose, thermoresponsive, hydrogel*

Introduction

Supramolecular assembly is growing into an established paradigm for the preparation of soft materials. The structural elements in supramolecular networks are held together due to physical cross-links driven by reversible non-covalent interactions such as hydrogen bonding, ionic or hydrophobic interactions, transition metal coordination, π-π stacking (Appel *et al.* 2012; Du *et al.* 2015; Sahoo *et al.* 2018; Voorhaar *et al.* 2016). The reversible and transient nature of such crosslinking enables the fabrication of environmentally responsive, self-healing, moldable soft materials. These attributes are highly desirable in various applications and actively explored in biomedicine, *e.g.* injectable hydrogels for tissue regeneration and drug delivery (Sahoo *et al.* 2018), food and cosmetic industries where encapsulation of bioactive ingredients is required (Zakharova *et al.* 2016) or for structuring and rheological modification (Zheng and Loh 2016), and the oil industry (Cao *et al.* 2015), *etc*.

Supramolecular networks can be built of low molecular weight substances (Du *et al.* 2015) or polymers (Voorhaar and Hoogenboom 2016). However, low molecular weight gelators tend to be complex molecules requiring challenging and costly synthesis. Moreover, the mechanical properties of (hydro)gels formed by small molecules are usually inferior compared to polymer-based counterparts. Polymer-based systems can utilize relatively simple chemical structures, with functional units randomly distributed along the macromolecule. They can also use more sophisticated macromolecular structures such as block co-polymers, polymers functionalized with complex motifs often inspired by biospecific interactions (Appel *et al.* 2012).

Hydrophobic interactions have been previously used for the improvement of strength and toughness of polymer hydrogels (Mihajlovic *et al.* 2017; Tuncaboylu *et al.* 2011) or as associative rheology modifiers in aqueous systems (Chassenieux *et al.* 2011; Lundberg *et al.* 1991). This latter approach is based on using copolymers with associative domains as a single hydrophobic block (in ABA-type

block copolymers), two end hydrophobic blocks (BAB-type block copolymer) or many randomly distributed hydrophobic groups (Chassenieux *et al.* 2011). Such amphiphilic copolymers assemble into a variety of morphologies *via* reversible hydrophobic interactions. Moreover, molecular association involving amphiphilic polymers is sensitive to temperature. This temperature dependence is due to entropically driven release of ordered/bound water at elevated temperatures when hydrophobic domains assembly into the aggregates. Therefore, hydrogels based on amphiphilic polymers provide a platform for the fabrication of reversible self-healing, thermoresponsive hydrogels where their rheology can be tuned from injectable formulations to tough and strong hydrogels.

Further alterations in mechanical properties of hydrogels and diversification of their functional properties can be achieved *via* the integration of nanoparticles into the hydrogel structure. Nanocomposite hydrogels is a thriving research field, and various nanoparticles have been explored as constituents of hybrid hydrogels. Reflecting the fact that hydrogels are aqueous systems, naturally most nanocomposite hydrogels have been developed with the use of hydrophilic nanoparticles such as clay minerals, nanocellulose, silica, graphene oxide (Alam *et al.* 2018; Schexnailder and Schmidt 2009). However, Baumann *et al.* (2010) reported an unexpected increase in stiffness of hydrogels based on a blend of hyaluronic acid and partially hydrophobic methylcellulose (MC) with the addition of hydrophobic nano- and microparticles made of poly (d,l-lactic-co-glycolic acid) (PLGA). The authors attributed such an effect to the hydrophobic interactions between MC and PLGA particles. Based on this observation, Appel *et al.* (2015) proposed the concept of making self-healing, thermoresponsive supramolecular and colloidal hydrogels *via* reversible association of soluble macromolecules and particles driven by hydrophobic interactions. To augment hydrophobic interactions, hydroxypropyl methylcellulose (HPMC) was modified using isocyanates with a long alkyl chain (hexyl, adamantyl and dodecyl). The most hydrophobic HPMC modified with dodecyl moieties allowed the formation of much stronger hydrogels in the presence of hydrophobic particles (polystyrene and PEG-*b*-PLA block copolymer). This confirmed that reversible networks can be built *via* transient hydrophobic interactions between amphiphilic polymers and nanoparticles. Such

hydrogels retained shear-thinning properties and quickly restored the network after shear deformation.

The current study further explores this concept using nanoparticles of high aspect ratio, cellulose nanocrystals (CNCs). To enable the formation of supramolecular and colloidal networks due to hydrophobic interactions, the surface of the CNCs is modified by binding hydrophobic octyl moieties (octyl-CNCs). HPMC was used as a soluble polymer with amphiphilic properties. Surface activity and thermal response of octyl-CNCs was confirmed by surface tension measurements. These all-cellulose supramolecular and colloidal systems are shear-thinning, temperature sensitive hydrogels of higher stiffness and strength compared to materials made with HPMC alone, and those containing only hydrophilic CNCs.

Materials and methods

Materials

Sodium metaperiodate, octylamine, hydroxypropyl methylcellulose (HPMC) with a molecular weight of approximately 86 kDa and viscosity of - 2,600-5,600 cP (2 wt% solution in water) were purchased from Sigma-Aldrich (Loughborough, UK) and used without further purification. Cellulose nanocrystals (CNCs) in sodium form were supplied as an 11.3 wt.% aqueous slurry by Maine University Process Development Centre (USA, Orono, ME). According to the manufacturer, the sulfur content of the CNCs was 0.9wt% sulfur per gram of dry CNCs.

Octyl-CNCs were synthesized according to the procedure described elsewhere (Nigmatullin *et al.* 2018). In short, the synthesis was made on a scale of 2.5 g CNCs. CNCs were oxidized by 0.9 g of KIO_4 for 24 hours. After, purification oxidized CNCs were reacted with 2.5 g of octylamine for 3 hours at 45 °C and for a further 21 hours at room temperature after adding $NaBH_3CN$. Octyl-CNCs were purified using centrifugation and finally dialyzed against deionized water. The suspension of purified octyl-CNCs was concentrated by allowing water evaporation through the dialysis membrane. Purified octyl-CNCs were kept as never-dried material as a concentrated gel.

Surface tension measurements

An advanced surface tensiometer from Krüss (Germany, model Krüss K100) was used for the measurements of surface tension. For the determination of the surface tension of CMC, a standard measuring probe (PL01) for the Wilhelmy plate method was used. Measurements at different CNC concentrations were performed by automatic serial dilutions using two micro dispensers (DS0810). The initial concentration of the octyl-CNC suspension was 7000 mg/L. 200 measurements were conducted, and the final concentration of octyl-CNCs was 10 mg/L. The CMC value was obtained using semi-log plot of surface tension against concentration. The influence of temperature on surface tension was studied in measurements using a rod-shaped probe (PL03) for the Wilhelmy method and a measuring vessel with capacity of 5 ml. HPMC solutions or octyl-CNC suspensions were heated to 80 °C. An aliquot of the hot solution was transferred into the measuring vessel and continuous measurements of surface tension were conducted for 20 minutes while the solution cooled down naturally. The instrument acquired surface tension values together with the corresponding temperature which was measured by an integrated temperature probe.

Rheological measurements

A Discovery HR-1 rotational rheometer (TA Instrument) equipped with a Peltier plate as a temperature controller was used for studying the rheology of the gels. A 'cone and plate' geometry used for the measurements consisted of a stainless steel cone of 40 mm diameter and angle 4°, and the Peltier plate. Frequency sweeps were conducted in strain controlled mode at 1.5 % strain and within an angular frequency range from 0.4 to 100 $rad \cdot s^{-1}$. The thermal response of the hydrogels was studied in an oscillation mode between 20 and 70 °C with a temperature ramp of 5° per minute using 1.5 % strain and an angular frequency 6.34 rad/sec. Additionally, flow curves were obtained at 20, 30, 40, 50 and 60 °C in steady shear within a shear rate range of 0.01 to 100 sec^{-1}. Amplitude sweeps were conducted at an angular frequency 6.34 $rad \cdot s^{-1}$, with oscillation strain variation between 0.01 to 650 %. During the rheological experiments, the measuring system was covered with a humidity chamber to minimize water evaporation.

NMR spectroscopy

HPMC solution and mixtures of HPMC/CNC 50/50 and HPMC/Octyl-CNC 50/50 with total solid content of 1 wt.% were prepared in D_2O (99.9 % ^2H) by overnight mixing of the corresponding amounts of the solid materials using a rotary mixer. Solution state NMR experiments were performed on a Bruker Avance I spectrometer equipped with a 5 mm probe, operating at a ^1H frequency of 499.69 MHz. Around 700 µL of sample were pipetted into a 5 mm NMR tube at room temperature. Variable temperature (VT) experiments were performed at 30, 40, 55 and 70 °C with 20 minutes thermal stabilization before acquisition. Representative spectra obtained at 30 °C are shown in Figure S1 of Electronic Supplementary Material.

To monitor the interactions of water (HDO) with hydrogel components upon heating, Saturation Transfer Difference (STD) NMR experiments (Mayer and Meyer 1999) were performed by selective ^1H saturation of the NMR-invisible core of cellulose network (0 ppm) (Calabrese *et al.* 2018). Cascades of 49 ms Gaussian-shaped pulses at a field strength of 50 Hz were employed, with a delay of 4 µs between successive pulses. The *on*- and *off*-resonance frequencies were set to 0 and 50 ppm, respectively, and a recycle delay of 6 s (including the saturation time) was used. The STD spectra were obtained by subtracting the *on*- from the *off*-resonance spectrum (I_{sat} and I_0, respectively). To determine the STD response (η_{STD}) of the HDO peak (which is indicative of the fraction of bound HDO), its signal intensity in the difference spectrum (I_{STD}) was integrated relative to the signal intensity in the *off*-resonance spectrum (I_0), and then by using the equation

$$\eta_{STD} = \frac{I_0 - I_{sat}}{I_0} \times 100 = \frac{I_{STD}}{I_0} \times 100 \qquad (1)$$

Different saturation times (t_{sat}; 0.5, 0.75, 1, 1.5, 2, 3, 4, 5 and 6 s) were used to obtain the STD build-up curve (STD(t_{sat}) *vs* t_{sat} (Figure S2 of Electronic Supplementary Material) which was then fitted to the monoexponential equation

$$STD(t_{sat}) = STD^{max}\left(1 - e^{(-k_{sat} * t_{sat})}\right) \qquad (2)$$

to derive the parameters STD^{max} and k_{sat}, which represent the asymptotic maximum of the build-up curve and the rate constant of the STD build-up, respectively. The initial slope of the STD build-up curve (STD_0) was calculated as the product of STD^{max} and k_{sat}, as shown in the equation

$$STD_0 = \frac{\partial STD(t_{sat})}{\partial t_{sat}}\Big|_{t_{sat}\to 0} = STD^{max} * k_{sat} \qquad (3)$$

The spectra were analyzed using TopSpin 3.5 software.

Results and discussions

Surface activity of gel components

It is generally recognized that nanocellulose (fibrils, nanocrystals) are amphiphilic nanoparticles due to exposure of less polar groups on some part of the crystals (Kalashnikova *et al.* 2012; Mazeau 2011). As a result, various forms of nanocellulose are efficient in the formation of Pickering emulsions (Kalashnikova *et al.* 2012). It appears that nanocellulose of lower surface charge are more amphiphilic since the efficiency in stabilizing emulsions improves for nanocellulose of low charge. In this work, commercially available CNCs were used. These were produced by hydrolysis in concentrated sulfuric acid and, as a result, they are highly charged (about 230 mmol $-SO_3^-$ per kg of CNCs). Surface tension measurements for CNCs suspensions with concentrations up to 8 g/L deviated from the surface tension of pure water within the error of measurement (data not shown). Thus, unmodified CNCs have very low surface activity. In contrast, hydrophobized octyl-CNCs significantly reduced surface tension (Figure 1) confirming the surface activity of hydrophobized materials through the attachment of octyl groups. The minimal value of surface tension attainable in octyl-CNC suspension was ~51 mN/m. As can be seen from Figure 1, there is a strong and linear dependence of surface tension on concentration for octyl-CNC suspensions with concentration up to approximately 2500 mg/L. This is typical for amphiphiles with concentration-dependent segments at low concentrations, and a region of constant surface tension at high concentrations. The onset of a steady-state value of surface tension is thought to be attributed to a critical micellar concentration (CMC) or more generally a critical aggregation concentration (CAC) when morphology of aggregates is not well defined. At this concentration, amphiphiles self-assemble

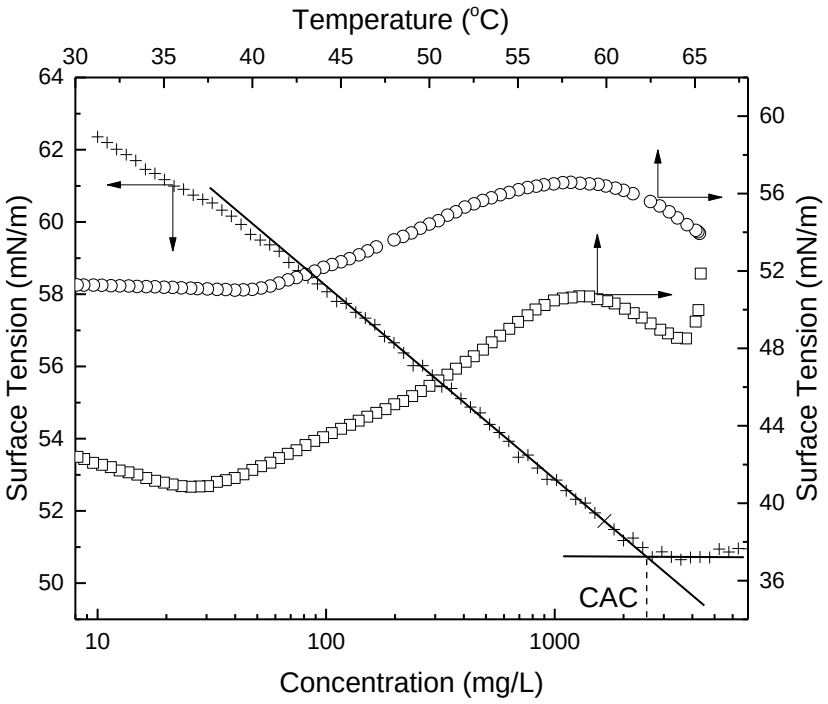

Figure 1: Dependence of surface tension of octyl-CNC suspensions (×, ○) and HPMC solution (□) on concentration (×) and temperature (○, □). HPMC and octyl-CNC concentration in the temperature dependence study was 500 mg/l. Solid lines are linear fittings of a plateau region and linearly dependent region proceeding the plateau. Critical aggregation concentration (CAC) determined as an intersection between these fitted lines.

into micellar or aggregated structures in the bulk of the solution (Chakraborty et al. 2011). The CAC for octyl-CNCs was found to be around 2500 mg/L.

Temperature induced association of amphiphiles can be probed by surface tension measurements. To exclude the interference from temperature effects on the size and structure of the dynamic micelles, the dependence of temperature on surface tension of octyl-CNC was studied using suspensions with a concentration of 500 mg/L, which is well below the CAC of octyl-CNCs. Only a small decrease in surface tension was observed with an increase of temperature to 40 °C (Figure 1). After this point, further temperature increases caused a gradual increase in the surface tension. Thus, the state of the octyl-CNCs in the suspension is sensitive to temperature. This indicates that the association of octyl-CNCs in the bulk of the suspension intensifies at temperatures above 40 °C. This association is thought to cause a decrease in the amount of amphiphilic particles at the air/liquid interface leading to a corresponding

increase in surface tension. The decrease in surface tension observed at temperatures above approximately 57 °C is likely to be due to a combination of two factors: i) a decrease in the surface tension with temperature characteristic for pure liquids; ii) the dissociation of micelles in the systems with higher thermal energy. To some extent a similar temperature response was observed for the solution of HPMC of the same concentration. HPMC causes a larger decrease in surface tension than octyl-CNC at the same concentration. Therefore, HPMC is characterized by a higher surface activity. Similar to octyl-CNC, there was an increase in the surface tension of HPMC between 35 and 57 °C which is evidence of the molecular association in the HPMC solution within this temperature range. Interestingly, unlike octyl-CNC suspensions, HPMC solutions underwent a sudden increase in surface tension when temperature approached 65 °C. At this temperature, extensive association of HPMC macromolecules led to a phase separation, which was noticeable visually as the turbidity of the solution increased dramatically. Thus, from surface tension measurements the temperature-sensitive behavior was observed for both HPMC and octyl-CNCs. It is worth summarizing that the association of these amphiphiles starts at relatively low temperatures (around 40 °C) and progresses gradually with an increase in temperature to 60 °C.

Gelation induced by reinforcing with nanoparticles

Rheology and reversible sol-gel transition for aqueous solutions of HPMC have been studied in detail (Haque *et al.* 1993; Joshi 2011; Silva *et al.* 2008). In line with the results of previous studies, the 4 wt% solution of HPMC used in this study showed a liquid-like behavior in oscillatory measurements at room temperature; in the low frequency zone G'' was higher than G' (Figure 2) and there was a sharper growth of G' ($G' \sim \omega^{1.17}$) compared to G'' ($G'' \sim \omega^{0.78}$). The curves intersected (G' = G'') at an angular frequency of ~40 rad^{-1}. Such a response is characteristic for an entangled polymer solution. However, HPMC solutions with half this concentration (2 wt%) were transformed to a system with G' dominant compared to G'', with the addition of an equal amount of CNC (total solid content 4 wt%). With a significant frequency dependence of both G' ($G' \sim \omega^{0.37}$) and G'' ($G'' \sim \omega^{0.44}$) HPMC solutions reinforced with CNCs can be defined as a weak gel. Similar effects of CNCs on the rheological properties of methylcellulose (MC), another water soluble thermoresponsive cellulose ether, has been previously reported (Hynninen *et al.*

(a)

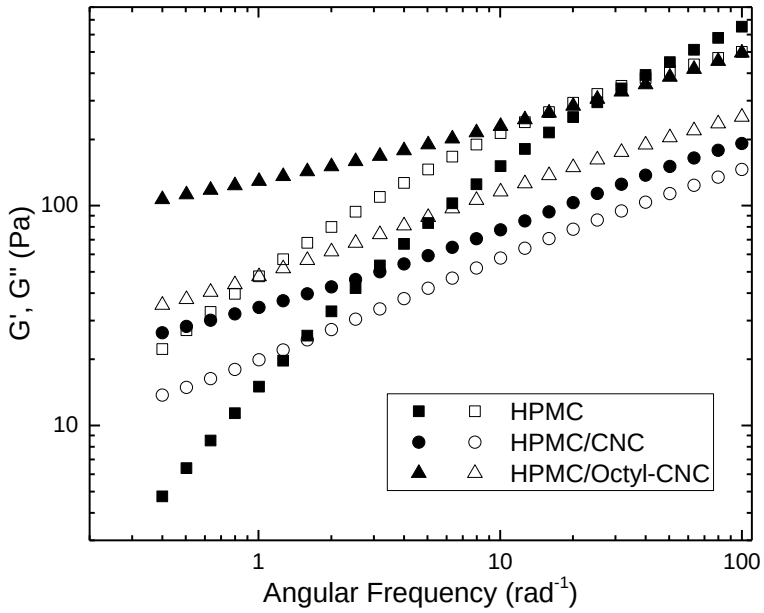

(b)

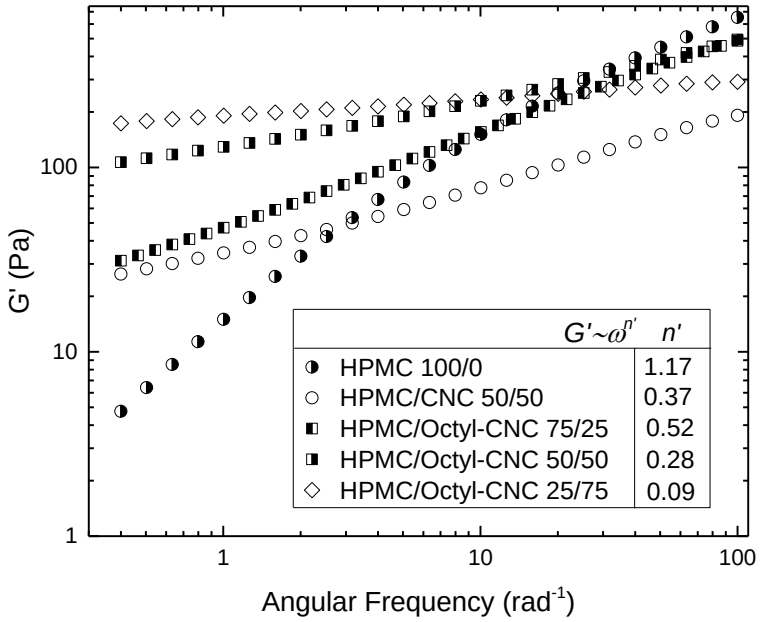

Figure 2: a) Comparison of mechanical spectra of HPMC hydrogel and hybrid hydrogels containing equal amounts of CNCs or octyl-CNC; b) the influence of frequency on G' for HPMC hydrogels and hybrid hydrogels of different compositions. Total solid concentration 4wt.%, numbers in compositions represent the mass ratio between HPMC and nanoparticles. Strain amplitude 1.5%.

2018; McKee *et al.* 2014). Using isothermal titration calorimetry, it has been shown that the enthalpy of mixing of MC and CNCs is highly negative, confirming an

affinity between MC and nanocellulose particles most likely due to hydrogen bonding and van der Waals interactions. This mechanism of formation of a hybrid polymer/nanoparticle network is expected to dominate at low temperatures for the systems with HPMC, since the hydrophilic components of these water-soluble polymers are similar.

As can be seen from Figure 2, further increase of hydrogel stiffness was observed when CNCs were replaced by hydrophobized octyl-CNCs. In hydrogels with octyl-CNCs instead of CNCs, both G' and G'' were less frequency dependent with $G' \sim \omega^{0.28}$ and $G'' \sim \omega^{0.37}$. Additionally, differences between G' and G'' increases in hydrogels with octyl-CNCs compared with hydrogels reinforced with CNCs. For example, at angular frequency of 1 Hz, G' was two times higher than G'' ($\tan \delta \approx 0.5$) in hydrogels with octyl-CNCs but 1.4 ($\tan \delta \approx 0.7$) times larger in the hydrogel with CNC. These observations indicate that the hybrid network formed by HPMC and octyl-CNCs is stronger which could be a result of an increased number of transient physical cross-links or/and an increased strength of interaction between the bridging soluble polymer and nanoparticles. This strongly suggests that association between hydrophobic domains of octyl-CNCs and HPMC modulates the stiffening of the hydrogels reinforced with particles according to the approach proposed by Appel *et al.* (2015).

Rheological properties of the hybrid supramolecular colloidal hydrogel are expected to depend on the polymer/nanoparticle ratio and the total solids concentration, which would allow formulating hydrogels with different rheological properties. In Figure 2b, frequency dependencies of G' as an indicator of hydrogel stiffness and strength are presented for several compositions. All hydrogels had the same solid content of 4 wt.%. The increase of octyl-CNC/HPMC ratio resulted in the enhancement of hydrogel stiffness accompanied with a lesser dependence on frequency (decrease in power low index (n) $G' \sim \omega^n$). Further evidence for the formation of a stronger network are obtained in large amplitude oscillatory shear (LAOS) experiments. Four types of G' and G'' response in LAOS experiments have been identified (Hyun *et al.* 2002): type I, strain thinning when both moduli decrease with the increase of strain; type II, strain hardening (increase of both modulus at larger strains); type III, weak strain overshoot (G' decreases with the

increase of strain while G'' increases in a certain range of shear followed by a decrease); type IV, strong strain overshoot (both moduli exhibit an increase in a certain strain range followed by a decrease). Figure S3a in Supplementary Material demonstrates that at 20 °C strain thinning (type I) was a characteristic of all hydrogels, except the HPMC/Octyl-CNC 25/75 hydrogel. The latter showed a segment of rising G'' followed by a decrease at larger strains. Such a response falls into type III; namely a weak strain overshoot. G'' indicates the energy dissipation due to a reorganization of the material's structure. The increase in G'' for the HPMC/Octyl-CNC 25/75 hybrid hydrogel implies that an additional energy is required for the distortion of the network structure which is in opposition to the flow. Thus, the hybrid network is the strongest among the studied compositions. When the network of HPMC/Octyl-CNC 25/75 hydrogel became fragmented by large deformations, a decrease in G'' is observed due to alignment of polymer chains and nanoparticles.

In addition to oscillatory measurements, the hydrogels were characterized in steady shear viscometry (Figure 3, Figure S4 Supplementary Material). As shown in Figure 3, all hydrogels demonstrated shear-thinning behavior reflecting the transient state of physical crosslinks. Generally, the Carreau model was a good fit to the experimental data acquired at 20 °C. This model is defined by the equation

$$\frac{\eta_{\dot{\gamma}}-\eta_{\infty}}{\eta_0-\eta_{\infty}} = \frac{1}{1+(K\dot{\gamma})^{1-n}}$$

where η_0 and η_{∞} are the zero-shear rate viscosity and an infinite shear rate viscosity, respectively, and K and n are fitting parameters. Figure 3 presents the fitted curves and corresponding values of the zero-shear rate viscosity for the hydrogels of several compositions. In line with the results of oscillatory measurements the zero-shear viscosity increased with an increasing content of octyl-CNCs in the hybrid hydrogels. The increase, of two order of magnitude or more, was observed for hybrid HPMC/Octyl-CNC 25/75 hydrogels compared with the pure HPMC hydrogels. A growing number of active junctions between HPMC molecules and octyl-CNCs with an increase of the nanoparticle content is thought to form more mechanically robust networks. This leads to higher values of shear viscosity.

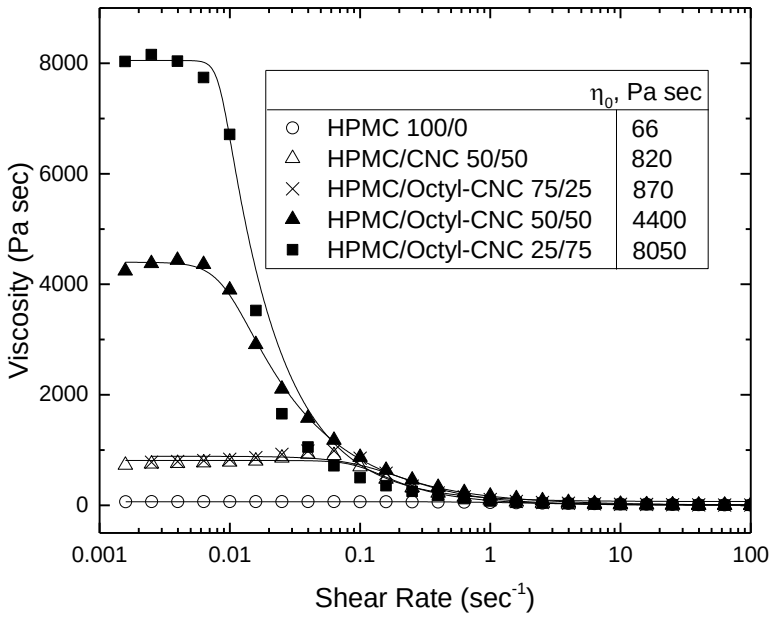

Figure 3: Typical flow curves for HPMC hydrogel and hybrid hydrogels with CNCs or octyl-CNCs of different compositions. The total solids concentration was 4 wt.%. The numbers given in the compositions represent the mass ratio between the HPMC and the CNCs. Solid lines are the Carreau model ($R^2 > 0.9$ for all compositions). Zero-shear viscosity is obtained from the fitted curves.

However, physical crosslinks are disturbed by the flow leading to their dissociation and consequently a drop in the viscosity with an increase in the shear rate.

Thermal response of hybrid hydrogels

It is well known that hydrophobic interactions are entropically driven, although that depends on the size of the solute. They are highly sensitive to temperature change, and as such should contribute to the variations in hydrogel properties with temperature. Thermal response of HPMC is well documented (Haque *et al.* 1993; Joshi 2011; Silva *et al.* 2008). In a temperature range between 50 and 70 °C two stages in the transformation of HPMC solutions have been identified: i) clustering of hydrophobic domains which is accompanied with the decrease in G'; ii) phase separation with the formation of interconnected polymer-rich regions and polymer-depleted regions. The system transforms into a gel state during the second stage, which manifests itself by sharp increase in G' during oscillatory rheometry. The change of G' with temperature obtained for the 4 wt.% HPMC solution (Figure 4) complies with these observations; G' gradually decreased with an increase in

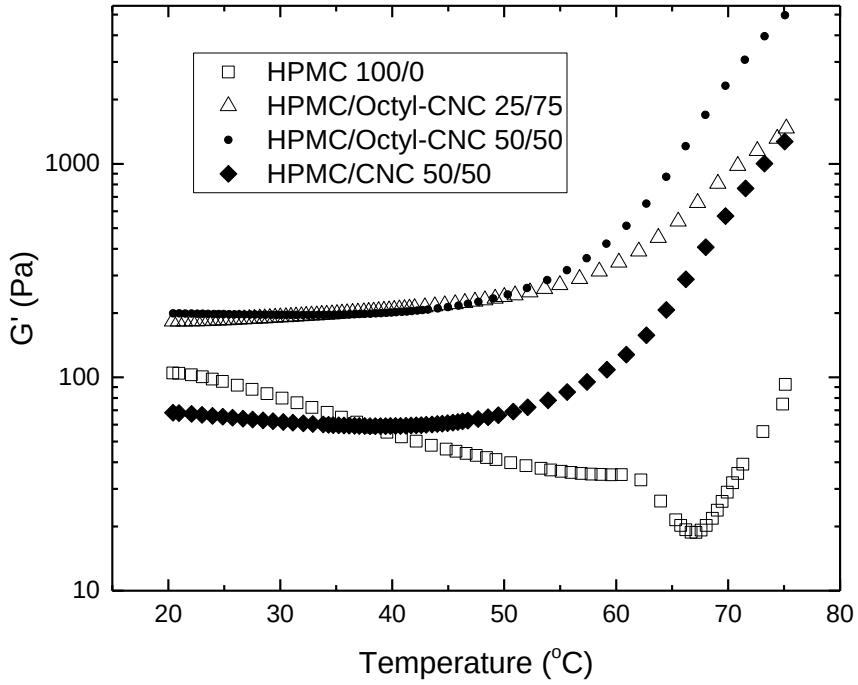

393

394 **Figure 4**: Variation of storage modulus as a function of temperature for HPMC and
395 hybrid hydrogels containing CNCs or octyl-CNCs. Total solids concentration was
396 4wt.%. The numbers shown in the compositions represent the mass ratio between
397 HPMC and the CNCs. Angular frequency was 6.28 rad sec^{-1} and the strain
398 amplitude was set at 1.5%.

399

400 temperature from 20 to 60 °C. Above 60 °C, an abrupt decrease in G' was observed
401 followed by sharp G' increase when the temperature exceeded 65 °C. However,
402 only a minor decrease in G' was observed for hybrid hydrogels with hydrophilic
403 CNCs in the temperature range between 20 and 50 °C. At the same time, G' was
404 found to increase even at low temperatures when hydrogel contained octyl-CNCs.
405 These observations further confirm the participation of nanoparticles in the
406 formation of a hybrid network structure.

407

408 The association of octyl-CNCs is likely to occur even at low temperatures, as was
409 demonstrated for the thermal response of surface tension. This effect combined with
410 hydrophobic interactions between octyl-CNCs and HPMC resulted in a continuous
411 increase in G' for the hybrid hydrogels containing octyl-CNCs. The most
412 significant changes in the rheological properties occurred at temperatures greater
413 than 55 °C. It appears that the onset of these changes is not affected by the type of

CNCs used; hydrophilic or hydrophobized CNCs. Over the whole temperature range, the association of HPMC and octyl-CNCs *via* hydrophobic interactions yielded hybrid hydrogels of higher stiffness compared to materials containing hydrophilic CNCs.

LAOS experiments at 50 °C, presented in Figure S3b of Supplementary Material, revealed type III response for HPMC/octyl-CNC hydrogels of 25/75 and 50/50 compositions while HPMC solutions and hybrid hydrogels with hydrophilic CNCs or low content octyl-CNC (HPMC/octyl-CNCs 75/25) remained strain thinning at elevated temperature. Thus, temperature induced association of HPMC in the solutions on its own, or in combination with hydrophilic CNC does not form strong enough structures to be detectable with an increase in G'. In contrast to low temperature (Figure S3a, Supplementary Material) HPMC/octyl-CNCs 50/50 showed an increase in G''. Notably higher increase in G'' for HPMC/octyl-CNCs 25/75 composition and transformation of HPMC/octyl-CNCs 50/50 into type III signify the effect of temperature on the strength of the hybrid network. The higher network strength causes more energy dissipation in LAOS at a shear which induces network disruption. Interestingly, for hydrogels with a higher octyl-CNC content (HPMC/Octyl-CNC 25/75) smaller increases in stiffness were observed at higher temperatures (Figure 4). It is probable that when the hydrogels contain a large fraction of octyl-CNCs the temperature induced self-association becomes dominant and a smaller number of physical crosslinks with HPMC are formed. This results in a less pronounced stiffening of the hydrogels with an increase of temperature. Thus, to obtain optimal properties of the hydrogels, the content of the soluble polymer and CNCs must be balanced depending on the temperature and hydrogel properties required for a specific application.

Flow curves also were obtained for the hydrogels at temperatures in the range 20 to 60 °C and are presented in Supplementary Material (Figure S4). Hybrid hydrogels exhibited a narrow shear thickening region at low shear rates, especially at elevated temperatures. (Note: the increase in viscosity is not obvious on all the curves due to the use of a log scale). Such a response to shear has been previously observed for some polyelectrolytes and the mechanism of this type of shear-thickening is not clear (Benchabane & Bekkour 2008). These data cannot be fitted using the Carreau

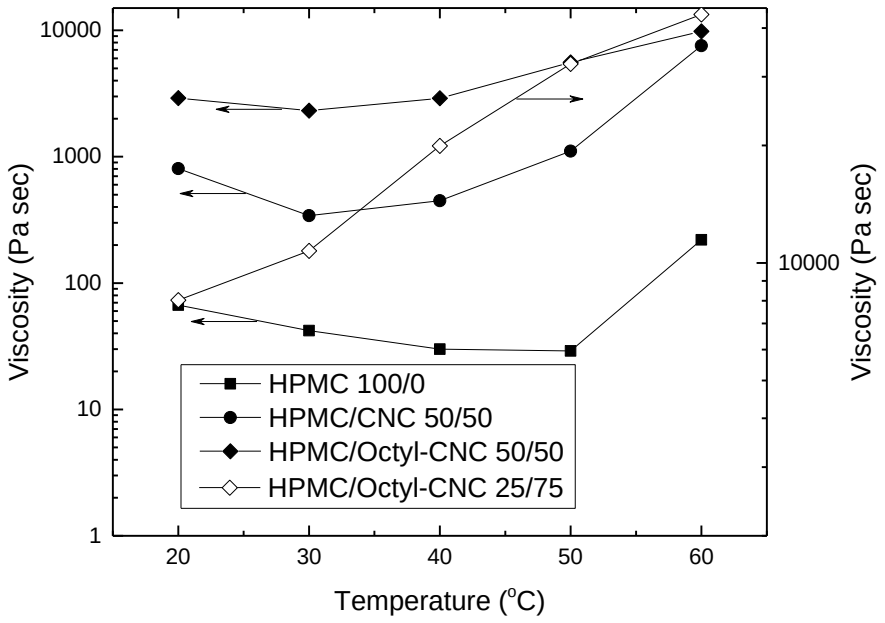

448

449 **Figure 5**: The influence of temperature on hydrogel viscosity at a shear rate of
450 0.015 sec^{-1}. Total solids concentration was 4wt.%. The numbers in the compositions
451 represent the mass ratio between HPMC and CNCs.

452

453 model. Therefore, in order compare the temperature effect on the viscosity of
454 hydrogels, Figure 5 presents results for viscosities taken from the flow curves in the
455 region of small shear; namely 0.015 sec^{-1}. Similar to changes in G', the viscosity at
456 this shear rate responded to temperature in a complex manner. A clear decrease in
457 viscosity was observed for the HPMC hydrogel and hybrid hydrogel containing
458 CNCs for temperatures up to 40 °C. This is thought to be a result of a commonly
459 seen decrease in a fluids' viscosity with an increase in temperature. Relatively small
460 reinforcement with hydrophilic CNCs cannot compete with this effect within the
461 low temperature range; viscosity starts increasing only when the association with
462 HPMC becomes significant at temperatures greater than 50 °C. However, when
463 hydrophobic octyl-CNCs are used, there was only a very small initial decrease in
464 viscosity for HPMC/octyl-CNC 50/50, while a steady increase in viscosity was
465 observed for HPMC/octyl-CNC 25/75.

466

467 Further insights into hydrogel structuring and thermal response were obtained from
468 Saturation Transfer Difference (STD) NMR spectroscopy experiments by assessing
469 binding of water to the hydrogel network (Calabrese *et al.* 2018). The analysis of
470 the STD initial slope (STD_0) of the residual water peak HDO (see Experimental

section) reports on the fraction of bound HDO (Figure 6). The gradual increase of the HDO STD_0 from 30 to 55 °C for mixtures of HPMC with both types of CNCs suggests an increased fraction of water bound by network upon heating (Figure 6), which qualitatively correlates with the increase in storage modulus (G') and viscosity (Figure 4 and 5, respectively). For the HPMC solution, however, the value of STD_0 of HDO decreases slightly from 30 to 55 °C, which might be associated with either a partial desolvation of macromolecules and/or less efficient spin diffusion at higher temperatures. It should be noted that the significant increase of the HDO STD_0 observed from 55 to 70 °C is due to the HPMC sample undergoing a sol-to-gel transition at around 65 °C (crossing of G' and G'', Figure S5 of Supplementary Material). Therefore, the increased fraction of network-bound water in the HPMC/CNCs and HPMC/Octyl-CNCs mixtures might be an important parameter to consider when explaining the growth of G' and viscosity upon heating. In that sense, it is relevant to note that the temperature dependence of HDO STD_0 is higher for HPMC/CNC than HPMC/Octyl-CNC hybrid hydrogels, or in other words, the fraction of network-bound water showed a higher increase for HPMC/CNC upon heating up to 70 °C (Figure 6). Moreover, HDO STD_0 was consistently lower for hydrogels incorporating hydrophobized octyl-CNCs compared with HPMC/CNC hydrogel. This decrease to a certain degree is likely to be defined by smaller area of hydrophilic surface for octyl-CNCs. However, association of hydrophobic domains in HPMC/octyl-CNC and subsequent water exclusion might also contribute to the decrease of bound water in HPMC/CNC systems. It is possible that HDO STD_0 decrease observed with the increase of temperature from 55 to 70 °C augmented this contribution due to extensive association of hydrophobic domains. Thus, the differences in the behavior of the HDO STD_0 between both hybrid hydrogels upon heating might result from a reduced water accessible surface area in the HPMC/Octyl-CNC network due to increased aggregation promoted by octyl-CNC hydrophobic interactions. This agrees with the much higher elastic behavior (G') of HPMC/Octyl-CNC within the whole temperature range (Figure 4).

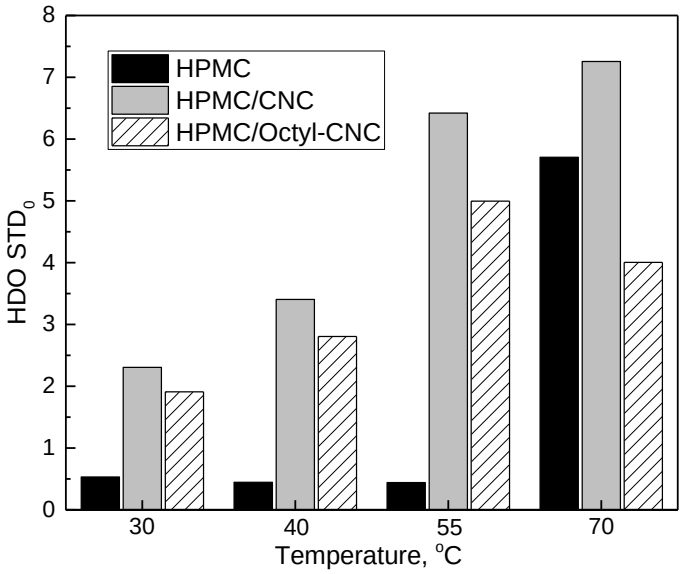

Figure 6: Bar chart showing the evolution of the STD_0 of the residual water peak (HDO) in HPMC solution, HPMC/CNC 50/50 and HPMC/Octyl-CNC 50/50 with total solid content 1 wt.% as a function of temperature, irradiating at 0 ppm (corresponding to the NMR invisible "core" of cellulose).

Conclusions

CNCs - high aspect ratio nanoparticles - were hydrophobized by surface binding of octylamine. Octyl-CNCs exhibited a typical amphiphilic behavior, decreasing surface tension in the aqueous suspensions. An increase in temperature of octyl-CNC suspensions induces growth in surface tension which indicates the intensification of self-assembly of octyl-CNCs in bulk of the suspension. Such properties of hydrophobized CNCs are prerequisite for recently conceptualized self-assembly of hybrid hydrogels *via* hydrophobic interactions between amphiphilic polymer and particles.

Both hydrophilic CNCs and octyl-CNCs reinforce HPMC solutions transforming them in self-supporting hydrogels with the elastic modulus dominating the loss modulus in oscillatory rheology. This implies that both types of CNCs were incorporated into the hybrid networks. However, hydrogels with octyl-CNCs are stronger, stiffer and more viscous compared with hydrogels containing hydrophilic CNCs. Thus, assembly of the water-soluble polymer and hydrophobized nanoparticles driven by hydrophobic interactions results in the formation of more robust hybrid network. The strength of network formed via association of

hydrophobic domains is further augmented at elevated temperatures as evidenced by a significant enhancement of rheological properties in both oscillatory rheology and steady shear viscometry. Rheological properties depend on the polymer/CNC ratio and temperature; compositions with the superior rheological properties observed at lower temperature might show inferior properties at higher temperatures. This was observed for compositions HPMC/octyl-CNC 25/75 and HPMC/octyl-CNC 50/50. Thus, polymer/octyl-CNC ratio must be balanced depending on the temperature and rheological properties required for a specific application. NMR spectroscopy revealed higher fraction of bound water in hybrid hydrogels compared with HPMC. The amount of network-bound water grows with the increase in temperature in parallel with the increase of hydrogel stiffness, strength and viscosity. This work expands the foundation for design of self-healing stimuli-responsive hybrid hydrogels with different rheological properties using assembly of amphiphilic polymers and nanoparticles driven by hydrophobic interactions.

Acknowledgments

The Engineering and Physical Sciences Research Council (EPSRC) is acknowledged for provision of financial support (EP/N03340X/2, EP/N033337/1). We are grateful for the use of the University of East Anglia (UEA) Faculty of Science NMR facility.

References

Alam A, Zhang Y, Kuan H-C, Lee S-H, Maa J (2018) Polymer composite hydrogels containing carbon nanomaterials—Morphology and mechanical and functional performance. Prog Polym Sci 77: 1-18. https://doi.org/10.1016/j.progpolymsci.2017.09.001

Appel EA, del Barrio J, Loh XJ, Scherman OA (2012) Supramolecular polymeric hydrogels. Chem Soc Rev 41: 6195–6214. DOI: 10.1039/c2cs35264h

Appel EA, Tibbitt MW, Webber MJ, Mattix BA, Veiseh O, Langer R (2015) Self-assembled hydrogels utilizing polymer–nanoparticle interactions. Nature Comm 6: 6295. DOI: 10.1038/ncomms7295

559 Baumann MD, Kang CE, Tator CH, Shoichet MS (2010) Biomaterials intrathecal
560 delivery of a polymeric nanocomposite hydrogel after spinal cord injury. 31:
561 7631-7639. doi.org/10.1016/j.biomaterials.2010.07.004
562
563 Benchabane A & Bekkour K (2008) Rheological properties of carboxymethyl
564 cellulose (CMC) solutions. Colloid Polym Sci 286: 1173-1180. DOI
565 10.1007/s00396-008-1882-2
566
567 Calabrese V, Muñoz-García JC, Schmitt J, Alves da Silva M, Scott JL, Angulo J,
568 Khimyak YZ, Edler KJ (2018) Understanding heat driven gelation of anionic
569 cellulose nanofibrils: combining STD NMR, SAXS and rheology. J Colloid
570 Interface Sci. *under consideration*
571
572 Cao P-F, Mangadlao JD, Advincula RC (2015) Stimuli-responsive polymers and
573 their potential applications in oil-gas industry, Polymer Rev 55:
574 706-733.https://doi.org/10.1080/15583724.2015.1040553
575
576 Chakraborty T, Chakraborty I, Ghosh S (2011) The methods of determination of
577 critical micellar concentrations of the amphiphilic systems in aqueous medium,
578 Arabian J Chem 4: 265-270. doi.org/10.1016/j.arabjc.2010.06.045
579
580 Chassenieux C, Nicolai T, Benyahia L (2011) Rheology of associative polymer
581 solutions. Curr Opin Colloid Interface Sci 16: 18–26.
582 doi.org/10.1016/j.cocis.2010.07.007
583
584 Du X, Zhou J, Shi J, Xu B (2015) Supramolecular hydrogelators and hydrogels:
585 From soft matter to molecular biomaterials. Chem Rev 115: 13165-13307.
586 https://DOI: 10.1021/acs.chemrev.5b00299
587
588 Haraguchi K (2007) Nanocomposite hydrogels. Curr Opin Solid State Mater Sci
589 11: 47–54. doi:10.1016/j.cossms.2008.05.001
590

591 Haque A, Richardson RK, Morris ER, Gidley MJ, Caswell DC (1993)
592 Thermogelation of methylcellulose. Part II: effect of hydroxypropyl substituents.
593 Carbohydr Polym 22: 175-186. https://doi.org/10.1016/0144-8617(93)90138-T
594
595 Hynninen V, Hietala S, McKee JR, Murtomäki L, Rojas OJ, Ikkala O, Nonappa
596 (2018) Inverse thermoreversible mechanical stiffening and birefringence in a
597 methylcellulose/cellulose nanocrystal hydrogel. Biomacromolecules 19:
598 2795-2804. DOI: 10.1021/acs.biomac.8b00392
599
600 Hyun K, Kim SH, Ahn KH, Lee SJ (2002) Large amplitude oscillatory shear as a
601 way to classify the complex fluids. J Non-Newtonian Fluid Mech 55: 51-65. Doi:
602 10.1016/S0377-0257(02)00141-6
603
604 Joshi SC (2011) Sol-Gel behavior of hydroxypropyl methylcellulose (HPMC) in
605 ionic media including drug release. Materials 4: 1861-1905;
606 doi:10.3390/ma4101861
607
608 Kalashnikova I, Bizot H, Cathala B, Capron I (2012) Modulation of cellulose
609 nanocrystals amphiphilic properties to stabilize oil/water interface.
610 Biomacromolecules 13: 267-275. 10.1021/bm201599j
611
612 Lundberg DJ, Glass JE, Eley RR (1991) Viscoelastic behavior among HEUR
613 thickeners. J Rheol 35: 1255–1274. doi.org/10.1122/1.550174
614
615 Mayer M, Meyer B (1999) Characterization of ligand binding by saturation transfer
616 difference NMR spectroscopy. Angew Chem Int Ed 38: 1784-1788.
617 doi.org/10.1002/(SICI)1521-3773(19990614)38:12<1784::AID-ANIE1784>3.0.C
618 O;2-Q
619
620 Mazeau K (2011) On the external morphology of native cellulose microfibrils.
621 Carbohydr Polym 84: 524-532. doi.org/10.1016/j.carbpol.2010.12.016
622

McKee JR, Hietala S, Seitsonen J, Laine J, Kontturi E, Ikkala O (2014) Thermoresponsive nanocellulose hydrogels with tunable mechanical properties. ACS Macro Lett 3: 266−270. dx.doi.org/10.1021/mz400596g

Mihajlovic M, Staropoli M, Appavou M-S, Wyss HM, Pyckhout-Hintzen W, Sijbesma RP (2017) Tough supramolecular hydrogel based on strong hydrophobic interactions in a multiblock segmented copolymer. Macromolecules 50: 3333–3346. doi: 10.1021/acs.macromol.7b00319

Nigmatullin R, Harniman R, Gabrielli V, Muñoz-García JC, Khimyak YZ, Angulo J, Eichhorn SJ (2018) Mechanically robust gels formed from hydrophobized cellulose nanocrystals. ACS Appl Mater Interfaces 10: 19318-19322. DOI: 10.1021/acsami.8b05067

Sahoo JK, Van den Berg MA, Webber MJ (2018) Injectable network biomaterials via molecular or colloidal self-assembly. Adv Drug Delivery Rev. 127: 185-207. doi.org/10.1016/j.addr.2017.11.005

Schexnailder P, Schmidt G (2009) Nanocomposite polymer hydrogels. Colloid Polym Sci 287: 1–11. DOI 10.1007/s00396-008-1949-0

Silva SMC, Pinto FV, Antunes FE, Miguel MG, Sousa JJS, Pais AACC (2008) Aggregation and gelation in hydroxypropylmethyl cellulose aqueous solutions. J Colloid Interface Sci 327: 333–340. doi:10.1016/j.jcis.2008.08.056

Tuncaboylu DC, Sari M, Oppermann W, Okay O (2011) Tough and self-healing hydrogels formed via hydrophobic interactions. Macromolecules 44: 4997-5005. DOI: 10.1021/ma200579v

Voorhaar L, Hoogenboom R (2016) Supramolecular polymer networks: hydrogels and bulk materials. Chem Soc Rev 45: 4013-4031. DOI: 10.1039/c6cs00130k

Zakharova L, Mirgorodskaya A, Gaynanova G, Kashapov R, Pashirova T, Vasilieva E, Zuev Yu, Synyashin O (2016) Supramolecular strategy of the

encapsulation of low-molecular-weight food ingredients. In: Grumezescu AM (ed), Encapsulations. Volume 2 Nanotechnology in the agri-food industry, Academic Press, pp 295-362.

Zheng YJ, Loh XJ (2016) Natural rheological modifiers for personal care. Polym Adv Technol 27: 1664–1679. https://doi.org/10.1002/pat.3822

Graphical Abstract